

# Even-odd alternative dispersions and beyond: Part I. Close oscillations on both sides of the (anti-)shock, quantum revival and fractalization

Jian-Zhou Zhu (朱建州)

*<sup>a</sup>Su-Cheng Centre for Fundamental and Interdisciplinary Sciences Gaochun Nanjing 211316 China*

---

## Abstract

Alternating the signs of the frequencies for Fourier components with even and odd (normalized) wavenumbers in the Korteweg-de Vries (KdV) equation maintains a dispersive shock with two-sided similar oscillations (like some plasma and quantum shocks). Such a modification, referred to as the even-odd-alternating KdV (aKdV) model, can also lead to fractalization and quantum revival (Talbot effect). Further refinement to introduce “boy-girl-twin” frequencies eliminates the disturbances on shock propagation caused by the even-odd asymmetry in the dispersion. Solitonic structures, including the shock as a “shoclon,” are prominently present. The traveling-wave solutions and on-torus invariants for quasi-periodic tori, for the Hamiltonian dynamics with the integrability structures broken (such as the loss of infinitely many invariants), are proposed to account for the (pseudo-)periodicity in the aKdV space-time patterns which correspond to presumably whiskered tori.

---

## 1. Introduction

The Korteweg-de Vries (KdV) equation as a “universal” model for the dynamics of many dispersive media in general admits marked oscillations on only one side of a shock, as evidenced by various results in the literature. This is natural, because dispersive waves originating from the shock are travelling unidirectionally according to the nature of the KdV dispersion.

Shocks of real physical systems however do often present genuine “two-sided” oscillations. For example, we can find such oscillations in the ion-acoustic shock waves observed in experiments [1] and in the one-dimensional particle-in-cell simulation results of Ref. [2] (with even-smaller-scale numerical noise, typical of such Lagrangian method, though). With a quantum nonconvex dispersion arising from the development of spin-orbit coupled Bose-Einstein condensates (BECs) [3, 4], they also appear in the quasi-one-dimensional dynamics [5], especially in their two-component Gross-Pitaevskii equation (GPE) simulations. These oscillations on the two sides appear to be not of that drastically different features in terms of wavelength and/or amplitude (see the nice accounts in Refs. [6, 7] for those produced by the Kawahara dispersions); they, in general, are neither from “external” forcing.

So, we propose the assignment of opposite-sign dispersions of the same order, which is accomplished in the KdV equation with periodic boundary condition by alternating the signs of the frequencies in the linear dispersion term for Fourier modes of even and odd (normalized) wavenumbers. Neighboring even and odd wavenumbers are of closest frequencies, so it is natural for us to think of separating and reflecting the dispersion sign of one class of them to account for similar oscillations on both sides of the shock, with such alternating KdV (aKdV) supporting bi-directional wave propagation. Subsequent even and odd wavenumbers are not really “twins”, so that the asymmetry between them can lead to effects that need to be corrected, which will be completed with the introduction of the “boy-girl-twin” dispersions.

On the other hand, the notion of soliton [8, 9, 10] and multi-soliton solutions, or the analogue in the periodic problem, acquires a kind of mathematical preciseness in the inverse scattering method in terms of

---

*Email address:* [jz@sccfis.org](mailto:jz@sccfis.org) (Jian-Zhou Zhu (朱建州))

the spectrum of the corresponding Lax-paired operator (see also, e.g., Refs. [11, 12] and references therein for, respectively, infinite-gap theory and the physical modeling of soliton gas with a special ansatz of the gap distribution in the large-gap-number limit); but, we use “soliton” in a more general sense, as already done in many studies of nonintegrable and even dissipative systems. Also fundamental is the fractalization and quantum revival (FaQR), associated to the Talbot effect, linear and nonlinear ([13, 14, 15, 16, 17, 18, 19] and references therein): at the linear level, the dynamics is already nontrivial [20]; and, although the inverse scattering method can in principle offer insights from the spectral properties for the corresponding initial data, at least numerically, in the integrable (such as the KdV and nonlinear Schrödinger) problems, FaQR works also in nonintegrable systems with limited understanding [21, 22]. “As the prevalence of allied effects continues to surprise, it is likely too early to attempt a clear mathematical definition” for FaQR “discovered and rediscovered several times since 1836” [23], according to the most recent work [24]. So, well-controlled models are needed to help shedding additional lights on such or more general structure-formation issues.

Linear waves of the same wavelength travelling oppositely can form standing-wave mode which might enhance the nonlinear interaction. This could be the reason causing the singularity of the Boussinesq equation, even in the “good” case:

$$u_{tt} = u_{xx} + (u^2)_{xx} - u_{xxxx} \quad (1.1)$$

whose Hamiltonian formulation, integrability and blow-up have been established [25, 26] (see Ref. [27] for a possible explanation between the formal paradox between the inverse-scattering linear problem and the original nonlinear blow-up). In Farmakis et al. [24], cubic nonlinearity is used to replace the quadratic nonlinearity in Eq. (1.1), showing non-Gibbs oscillations and even somewhat strong spikes. We will also see strong spikes in some of aKdV results. No evidence of blow-up have been clearly obtained, which remains for further studies. Here, our focus is on the discovery and its possible reason of the emergence of (pseudo-)periodic patterns with shocks of two-sided similar oscillations from such presumably nonintegrable systems.

Below, we will introduce in Sec. 2 the even-odd alternation of dispersions, and, the variational and Hamiltonian formulation, with particularly the discussions of on-torus invariants and quasi- and almost-periodic tori, and, FaQR. Sec. 3 contains the basic numerical analyses and tentative physical applications in modeling the ion-acoustic shocks, including both the cases with sinusoidal and step-function initial data and, correspondingly, the respective (dispersive) shock formation and FaQR. Sec. 4 concludes the work with expectations.

## 2. Theoretical formulation

We start with the KdV equation

$$\partial_t u + u \partial_x u + \mu \partial_x^3 u = 0 \quad (2.1)$$

which, in a periodic interval of length  $L_p$  normalized to be  $2\pi$  for convenience of theoretical formulation, reads in Fourier  $k$ -space

$$(\partial_t - \mu \hat{i} k^3) \hat{u}_k + \hat{i} \sum_{p+q=k} q \hat{u}_p \hat{u}_q = 0 : \quad (2.2)$$

with the Fourier coefficient

$$\hat{u}_k(t) = \int_0^{2\pi} u(x, t) \exp\{-\hat{i} k x\} dx / (2\pi) =: \mathcal{F}\{u\}(k, t) \quad (2.3)$$

with  $\hat{i}^2 = -1$  and the complex conjugacy  $\hat{u}_k^* = \hat{u}_{-k}$  for real  $u$ ,

$$u(x, t) = \sum_k \hat{u}_k \exp\{\hat{i} k x\} =: \mathcal{F}^{-1}\{\hat{u}_k\}(x, t) \quad (2.4)$$

with appropriate properties depending on our requirements on the behaviors of the series (in general, we assume convergence, thus simply the equality with the Fourier expansion, but for special cases involving

discontinuities, such as the FaQR below, slightly more careful usage of the notation will be applied for caveat).

In this note, we will be studying the aKdV equation,

$$\partial_t u + u \partial_x u + \mu \partial_x^3 \left[ \mathcal{F}^{-1} \{ \text{mod}(k+1, 2) \mathcal{F}\{u\}(k) \} - \mathcal{F}^{-1} \{ \text{mod}(k, 2) \mathcal{F}\{u\}(k) \} \right] = 0 \quad (2.5)$$

with  $\text{mod}(k, 2) = [(-1)^k + 1]/2$ , and its further variations.

### 2.1. The definitions and equations

The modification of the dispersion term in Eq. (2.5) of the KdV dispersion  $\hat{D}_k = -\hat{i}\mu k^3 \hat{u}_k$  is, put in words, simply separating the even and odd- $k$  modes and reverse the sign of the dispersion of one of the branches with appropriate assumptions of the Fourier series; that is,

$$\hat{D}_k = (-1)^{\text{mod}(k, 2)} \hat{i} \mu k^3 \hat{u}_k \quad (2.6)$$

which is really what will be used below. But, for slight generalization and for a glance at its formulation in physical space, some more tedious but trivial elaborations (mostly just for introducing some more notations for later usage) of the implicit pseudo-differential operators involved follow.

In  $x$ -configuration space, the more general even-odd separation of the dispersion term  $D$  is modified to be  $\tilde{D} = {}^e\tilde{D} + {}^o\tilde{D}$ , where

$${}^e\tilde{D}(x) = -\hat{i} {}^e\mu \sum_k (2k)^3 \hat{u}_{2k} \exp\{\hat{i}2kx\} = -\hat{i} {}^e\mu \sum_k k^3 {}^e\hat{u}_k \exp\{\hat{i}kx\} = {}^e\mu \partial_x^3 {}^e u, \quad (2.7)$$

with  ${}^e\hat{u}_k := \text{mod}(k+1, 2)\hat{u}_k$ ; and, similarly for the odd component,

$${}^o\tilde{D} = -\hat{i} {}^o\mu \sum_k (2k+1)^3 \hat{u}_{2k+1} e^{\hat{i}(2k+1)x} = -\hat{i} {}^o\mu \sum_k k^3 {}^o\hat{u}_k \exp\{\hat{i}kx\} = {}^o\mu \partial_x^3 {}^o u, \quad (2.8)$$

with  ${}^o\hat{u}_k := \text{mod}(k, 2)\hat{u}_k$ . That is, we have

$$\partial_t u + u \partial_x u + ({}^e\mu \partial_x^3 {}^e u + {}^o\mu \partial_x^3 {}^o u) = 0 \quad (2.9)$$

with

$${}^e u = \mathcal{F}^{-1} \{ \text{mod}(k+1, 2) \mathcal{F}\{u\} \} \text{ and } {}^o u = \mathcal{F}^{-1} \{ \text{mod}(k, 2) \mathcal{F}\{u\} \}, \quad (2.10)$$

as used in Eq. (2.5); or, in  $k$ -space, the dispersion function  $\omega(k)$  in Eq. (2.6),  $\hat{D}_k = \Omega(k)\hat{u}_k$ , being slightly generalized,

$$\partial_t \hat{u}_k - \hat{i} \Omega(k) \hat{u}_k + \hat{i} \sum_{p+q=k} q \hat{u}_p \hat{u}_q = 0 \quad (2.11)$$

with

$$\Omega(k) = k^3 [{}^e\mu \text{mod}(k+1, 2) + {}^o\mu \text{mod}(k, 2)]. \quad (2.12)$$

${}^e\mu$  and  ${}^o\mu$  may be chosen to be independent, but we will start with  $\mu = {}^e\mu = -{}^o\mu$  (thus the conventional KdV dispersion  $D = {}^e\tilde{D} - {}^o\tilde{D}$ ) which is used in the numerical analysis in Sec. 3.

### 2.2. The variational principle and Hamiltonian formulation

As directly discernable, Gardner's [28] KdV formulation in  $k$ -space can be carried over for aKdV, but for convenience of further theoretical discussions on travelling waves and invariant tori, we formally lay out the similar results in  $x$ -space.

Obviously, for any variable  $v$ , the operators  $\mathcal{E} : v \rightarrow {}^e v$  and, similarly,  $\mathcal{O}$  are *linear*, satisfying

$$\mathcal{E}\mathcal{E} = \mathcal{E}, \quad \mathcal{O}\mathcal{O} = \mathcal{O} \text{ and } \mathcal{E}\mathcal{O} = \mathcal{O}\mathcal{E} = \mathcal{N} : v \rightarrow 0, \quad (2.13)$$

and, *commutativity* with respect to the differentiation operators. And just as the derivatives of  $v$ ,  ${}^{e/o}v$  should be treated as independent variables derived from  $v$  in functional calculations. The variation of  ${}^{e/o}v$  comes from that of  $v$ . Introducing  $\phi$  with  $\phi_x = u$  (thus  ${}^{e/o}\phi_x = {}^{e/o}u$  — subscripts for  $\phi$  denoting partial differentiations), we have the least-action variational principle

$$\delta \int L dx dt = 0 \quad (2.14)$$

with the Lagrangian density

$$L = \phi_x \phi_t / 2 + \phi_x^3 / 6 - {}^e\mu ({}^e\phi_{xx})^2 / 2 - {}^o\mu ({}^o\phi_{xx})^2 / 2, \quad (2.15)$$

which gives Eq. (2.9) through the Euler equation

$$\frac{\partial}{\partial t} \frac{\partial L}{\partial \phi_t} + \frac{\partial}{\partial x} \frac{\partial L}{\partial \phi_x} - \frac{\partial^2}{\partial x^2} \left( \frac{\partial L}{\partial {}^e\phi_{xx}} + \frac{\partial L}{\partial {}^o\phi_{xx}} \right) = 0. \quad (2.16)$$

[The above equation can be derived by introducing a  $\phi$  variation (which causes the corresponding variations of  ${}^e\phi_{xx}$  and all that functions in  $L$ ) and perform the standard direct computations, with the application of the properties (especially the *linearity* and *commutativity* with respect to differentiations) of the operators  $\mathcal{E}$  and  $\mathcal{O}$ , and,  $\mathcal{F}$  and  $\mathcal{F}^{-1}$  in Eq. (2.10).] Actually, we may define the Hamiltonian

$$\mathcal{H} = \int_0^{2\pi} [{}^o\mu (\partial_x {}^o u)^2 / 2 + {}^e\mu (\partial_x {}^e u)^2 / 2 - u^3 / 6] dx, \quad (2.17)$$

with the even and odd velocities given in the above through the Fourier expansion of  $u$  after Eqs. (2.7) and (2.8) respectively. We can directly verify, with Eq. (2.11), that

$$\frac{d\hat{u}_k}{dt} = \frac{\hat{i}}{2\pi} k \frac{\partial \mathcal{H}}{\partial \hat{u}_k^*}. \quad (2.18)$$

We can also verify

$$\partial_t u = \{u, \mathcal{H}\} = \frac{\partial}{\partial x} \frac{\delta \mathcal{H}}{\delta u} \quad (2.19)$$

with Hamiltonian operator  $\partial_x$  and the *Poisson bracket*

$$\{\mathcal{F}, \mathcal{G}\} = \int_0^{2\pi} \frac{\delta \mathcal{F}}{\delta u} \frac{\partial}{\partial x} \frac{\delta \mathcal{G}}{\delta u}. \quad (2.20)$$

In other words, with only the change of the linear dispersion term, much of the classical KdV carries over, *mutatis mutandis*.

We note that the decomposition and assignment of dispersion, and, the above variational principle and Hamiltonian formulation hold actually for quite “arbitrary” grouping and linear dispersion-assignment (except for some possibly exotic ones which might lead to mathematical difficulties) of the Fourier modes and can be carried over to continuous- $k$  case (for unbounded domain) by working with the intervals, say,  $(I - 0.5, I + 0.5]$  for integer  $I$ s. As indicated, the models such constructed is not expected to simulate some type of physical problems universally for all kinds of initial and boundary conditions, but rather to help exposing and understanding some dynamical mechanisms in specific situations.

Further possibility of the structures in this line with the spirit of Lie’s theory and others deserves futher examination and is left for future studies. Here, in the following two sub-sections, we merely discuss in such a context the travelling waves and quasi-periodic solutions, akin to the relevant theories of the periodic KdV problem [29, 30].

### 2.2.1. Travelling waves

The periodic KdV cnoidal wave, as the name suggest, already takes the nontrivial mathematical form (Jacobi elliptic function). With the somewhat complex pseudo-differential operator involved, the corresponding aKdV travelling wave probably can not be explicitly expressed by a known function, but for convenience writing, let us call it “shnoidal wave” associated to the function (say, denoted by “shn” in which “sh” might be connected to the “shocliton” below) to be specified as follows. The wave of velocity  $\lambda_1$  corresponds to the special solution to Eq. 2.11, with

$$\partial_t \hat{u}_k = \hat{i} k^3 [{}^e \mu \bmod (k+1, 2) + {}^o \mu \bmod (k, 2)] \hat{u}_k - \hat{i} \sum_{p+q=k} q \hat{u}_p \hat{u}_q = -\hat{i} \lambda_1 k \hat{u}_k. \quad (2.21)$$

Actually, it is direct to check that still two more of the KdV invariants,

$$\mathcal{E} = \int_0^{2\pi} u^2 dx \text{ and } \mathcal{M} = \int_0^{2\pi} u dx, \quad (2.22)$$

are conserved accordingly by aKdV. That is,

$$\{\mathcal{E}, \mathcal{H}\} = 0 = \{\mathcal{M}, \mathcal{H}\}. \quad (2.23)$$

So, we see that the above shnoidal wave can be realized by the critical set of the KdV flow specified by

$$\frac{\delta \mathcal{H}}{\delta u} - \lambda_1 \frac{\delta \mathcal{E}}{\delta u} = 0. \quad (2.24)$$

Whether including  $\mathcal{M}$ , vanishing or not, does not matter here, as in KdV [29, 30].

Note that, introducing the Galerkin truncation, i.e., keeping only modes of a finite set of wavenumbers, makes it possible to write down some explicit solutions to Eq. (2.21), just as in other models [31], which however is not the purpose here.

### 2.2.2. On-torus invariants

No other aKdV invariants beyond  $\mathcal{H}$ ,  $\mathcal{E}$  and  $\mathcal{M}$  can be found so far. However, as we will see below, similar multi-soliton analogue like the KdV case presents in aKdV numerical results with periodic boundary condition, which somehow calls for a setup resembling the infinitely many invariants of the integrable KdV.

Actually, for any integral functional  $\mathcal{I}_\tau$  ( $\mathcal{I}_1 = \mathcal{E}$ ) defining the tori by the critical sets of the aKdV flow with

$$\frac{\delta \mathcal{H}}{\delta u} - \sum_{\tau} \lambda_{\tau} \frac{\delta \mathcal{I}_{\tau}}{\delta u} = 0, \quad (2.25)$$

it is straightforward to show the on-torus invariance, i.e.,  $d \sum_{\tau \neq 1} \lambda_{\tau} \mathcal{I}_{\tau} / dt = 0$ , or  $\{\sum_{\tau \neq 1} \lambda_{\tau} \mathcal{I}_{\tau}, \mathcal{H}\} = 0$ . Chosen to be mutually Poisson commuting (if possible), each  $\mathcal{I}_{\tau}$  then should Poisson commute with  $\mathcal{H}$ , so that

$$d\mathcal{I}_{\tau}/dt = \{\mathcal{I}_{\tau}, \mathcal{H}\} = 0, \quad (2.26)$$

i.e., on-torus invariance indivisually. [The KdV integral invariants mutually Poisson commute [28], but here  $\mathcal{I}_{\tau}$  can be quite arbitrary, thus not commuting unless chosen to be so.] This way, it could be possible to have solutions to Eq. (2.21) with the right hand side replaced by more general  $\hat{i} \omega(k) \hat{u}_k$ , thus the possibility of quasi- or even almost-periodic tori.

Then we would have a setup resembling that for the KdV finite-gap theory, though we do not know the corresponding operator, not even for its existence, as in that KdV Lax pair. Nevertheless, we tend to believe that such on-torus-invariance scenario is relevant to the numerical results to be presented, which might be generic for (nonintegrable)<sup>1</sup> conservative systems associated to the concept of pseudo-integrability [31, 32].

---

<sup>1</sup>We use the term “(non)integrable” in the popular sense associated to the inverse scattering method, but, actually, the meaning of integrability by itself is not really clear and is a subject of research.

The latter notion is defined through the patterns, to be discovered numerically, with solitonic structures accompanied by (much) weaker disordered components, indicating the (statistically) stable whiskered tori. Each such torus carries a set of invariants specific to it. For each realization, finding out the “right” on-torus invariants can be challenging, but not necessarily completely untraceable. For example, each Hamiltonian flow  $u_t = \partial_x \frac{\delta \mathcal{I}}{\delta u}$  should reflect some aspect(s) of the structure of the tori or the physical feature (such as some kind of symmetry).

### 2.3. Remarks on the dispersion, shock and oscillations

We will see that the dispersive quantization and fractalization, leading to pulses from, say, piecewise constant data corresponding to the physical (anti)shocks, are consistent with the oscillation scenario.

#### 2.3.1. Linear dispersion and dispersive quantization/fractalization

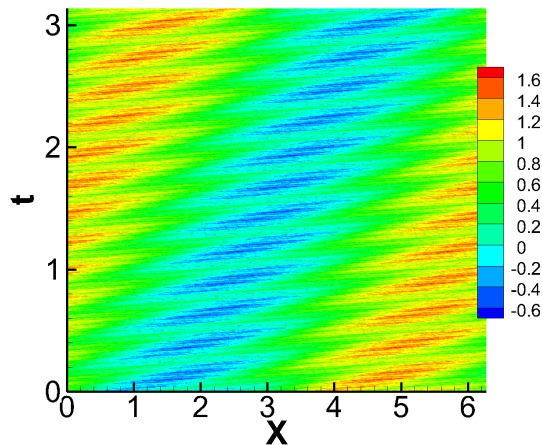


Figure 1: LaKdV space-time contours/carpet from the simple step-function initial data (2.28), with  $\varrho\mu = 1 = -e\mu$ .

Without the nonlinear advection/dispersion term, we can write down the solution,

$$u(x, t) \sim \sum_k \hat{u}_k(t) e^{ikx} \text{ with } \hat{u}_k(t) = \hat{u}_k(0) e^{i\Omega(k)t}, \quad (2.27)$$

to the Cauchy problem of the linear dispersion, here the linearized aKdV (LaKdV) modifying the linearized KdV (LKdV), but the result is highly nontrivial or bizarre, presenting FaQR which have rich physical and mathematical background, tracing back to the Talbot effect, both linear and nonlinear, and extending to many models [13, 16, 18, 17, 21, 22, 20, 24]. From the various familiar dispersion functions, of polynomials or not [21, 24], besides our  $\Omega$ , the problem is clearly of number-theoretic feature for the characters of  $u(x)$  with  $t$  being rational or irrational (relative to  $\pi$ ). Our angle of view is slightly of dynamical nature, i.e., more concerned by how the structures or patterns are driven or formed, although further manipulations of the dispersion function appear useful for number-theoretic studies along this line in the future.

We start with the unit-step-function initial data

$$u(x, 0) = \begin{cases} 0, & 0 < x < \pi, \\ 1, & \pi < x < 2\pi. \end{cases} \text{ or, } \hat{u}_k(0) = \begin{cases} \frac{i}{\pi k}, & k \text{ odd,} \\ \frac{1}{2}, & k = 0, \\ 0, & k \neq 0 \text{ even.} \end{cases} \quad (2.28)$$

The values at the discontinuity locations, also for the case in Fig. 2, are not essential, but are taken to be the average,  $1/2$ , consistent with the Fourier analysis [18]. The corresponding results of Refs. [18, 20]), with

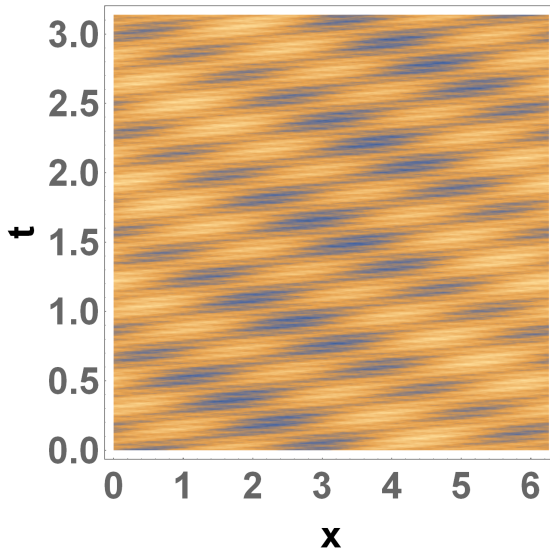


Figure 2: LaKdV space-time contours/carpets from  $u(x, t) = 0$  for  $x/(2\pi) \in (0, 1/8) \cup (3/8, 1/2)$ ,  $= 1$  for  $x \in (1/8, 3/8) \cup (1/2, 1)$ , with  ${}^o\mu = 1 = -{}^e\mu$ .

${}^o\mu = 1$ , carry over with no necessity of any change, because modes of even  $k \neq 0$  are vanishing, resulting in no differences between KdV and aKdV evolution, as shown in Fig. 1, also given in Ref. [18] but with more remarks offered a bit later.

Actually, the following theorem for LKdV has been established [18, 20]:

**Theorem 1.** *Let  $\frac{p}{q} \in \mathbb{Q}$  be a rational number with  $p$  and  $q$  having no common factors. Then the solution to the initial-boundary value problem at time  $t = \pi \frac{p}{q}$  is constant on every subinterval of the form  $\frac{\pi j}{q} < x < \frac{\pi(j+1)}{q}$  for  $j = 0, \dots, 2q - 1$ .*

**Remark 1.** *The proof in Ref. [18] is based on the expression of the Fourier expansion of  $u(x, t)$  itself. We feel that it can be more intuitive to prove the above theorem, and similarly also relevant results in Ref. [20] on the characterization of the region of constancy, by computing  $\partial_x u(x, t)$  and analyzing the vanishing or nonconvergent conditions, which can also be carried over, mutatis mutandis, to establish the corresponding analytical results for our LaKdV here (with the Weyl and Kummer sums etc. changed accordingly). However, since there is no essential differences in the mathematical nature, we defer such otherwise boring discussions to another communication concerning the effects on particle transports which are sensitive to such details as shocks, oscillations and fractals. Actually, as will be remarked again, our nonlinear aKdV results are also in a sense close to those of KdV, with differences though. So, focusing on the shock-antishock structure and the associated oscillations, we do not bother such detailed quantitative differences here. Presenting the scenario is sufficient for our purpose here.*

Related to our theme of dispersive (anti)shocks and oscillations, the major wave with  $|k| = 1$  travels with unit velocity, as can be seen directly from the overall tilted pattern in the carpet of Fig. 3, right panel. Olver [18] noticed such “discernible wave that moves across the interval with unit speed”. Actually, all details can be explained by the wave velocity  $\Omega(k)/k = k^2$ : the wave of  $|k| = 3$  is responsible for the intermediate tilted stripes of red and blue (separated by green) colors whose slope/velocity (reciprocal) is seen to be  $1/9$ , and fine bands inside each stripe corresponding to the wave of  $|k| = 4$  of slope  $1/16$  are also visible with our bare eyes. The pattern looks, very roughly, like the dispersive (anti)shock, and we will see in Sec. 3.4 that such linear dynamical features persist in the nonlinear regime with well preserved shock-antishock structure from the initial data.

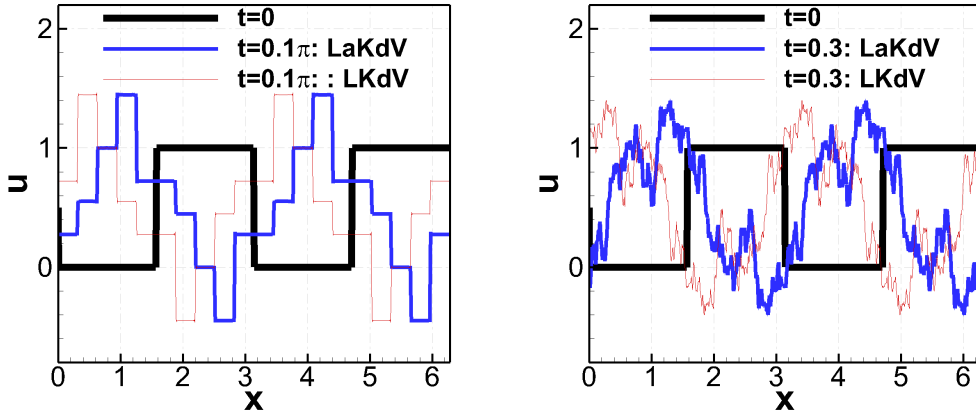


Figure 3: The comparison of LaKdV and LKdV quantized (left) and fractal (right) profiles at, respectively, rational and irrational times (with respect to  $\pi$ ).

The quantization/fractalization features extend to other initial piecewise-constant data, as partly shown in Fig. 3, starting from a piecewise-constant data at the initial time  $t = 0$  with  $\mu = \circ\mu = 1 = -\epsilon\mu$ .

How LaKdV differs from LKdV of course depends on the initial data. Although, except for the locations, it is hard to detect with bare eyes any essential differences in the fine structures in Fig. 3 between LaKdV and LKdV, the associated number-theoretic aspect [20] shall be different and preliminary numerical tests show they in general are different in the shocks and fractals, resulting in amplified differences in the transports of particles. Also, just as the persistence of different rivals and fractalization in other nonlinear models, the corresponding persistence of fractalization and quantization should be expected in our aKdV. It is expected the differences between the aKdV and KdV dynamics would have interesting consequences on particle (density) transports.

In any case, we have seen that quantization and fractalization still (very) roughly keeps the shocks (or probably closer to “undular bores”), introducing “oscillations”, quantized or fractal.

### 2.3.2. Correcting the neighboring asymmetry

In our even-odd alternating-sign model, the asymmetry effect between even and odd wavenumbers increases with the decrease of the wavenumber. This is intuitively obvious: the relative difference between wavenumber  $n = 1$  and 2 should be larger than that between 10 and 11, say, just as their relative differences of the values of the wavenumbers. To correct such an asymmetry and have a “boy-girl twins”, we can further replace the adjacent wavenumbers  $k = 2m$  and  $k = 2m - \text{sgn}(m)$  in the dispersion (2.12) with the same  $k = 2m - \text{sgn}(m)/2$ . That is,  $\Omega(2m) \rightarrow \Omega(2m - \frac{\text{sgn}(m)}{2}) \leftarrow \Omega(2m - \text{sgn}(m))$ , i.e.,

$$\Omega(k) = \hat{i}[k + \text{sgn}(k) \bmod(k, 2) - \frac{\text{sgn}(k)}{2}]^3 [\epsilon\mu \bmod(k+1, 2) + \circ\mu \bmod(k, 2)]. \quad (2.29)$$

Such a correction of the linear term does not affect the conservation laws and variational formulation, and we will see that the shock propagation indeed can be nicely corrected (Fig. 9 below).

## 3. Numerical analysis

### 3.1. Even-odd decompositions

Note that the KdV even/odd dynamics

$$\epsilon/\circ\partial_t u + \epsilon/\circ(u\partial_x u) + \epsilon/\circ\mu \epsilon/\circ\partial_x^3 u = 0, \quad (3.1)$$



which can be obtained by simply collecting from Eq. (2.2) the even/odd modes, are “non-symmetric” in the sense that triadic interactions in  ${}^{e/o}(\hat{i} \sum_{p+q=k} q \hat{u}_p \hat{u}_q)$  corresponding to the nonlinear term are composed of the “even-even”, “even-odd” and “odd-odd” ones which result in, non-symmetrically, “even”, “odd” and “even”  $k$ , respectively. For example, we may remove all the odd- $k$  modes to have pure even-dynamics, but there is no nonlinear pure odd-dynamics.

Following ZK65, we performed simulations with the same setup as theirs, that is, starting from the initial longest-wavelength profile  $u_0 = \cos(\pi x)$  and performing the direct numerical simulation with periodic boundary condition over  $[0,2)$ , but now with the standard pseudo-spectral method;  $\mu = \delta^2$  with  $\delta = 0.022$  in Eq. (2.1).

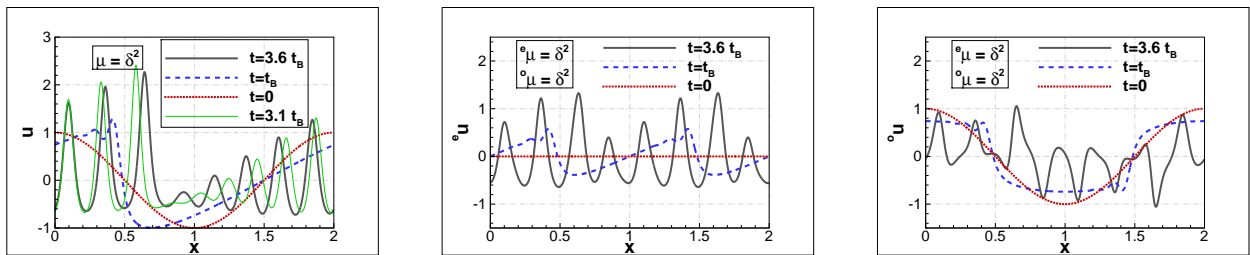


Figure 4: The KdV  $u$  (after ZK65) and the corresponding even and odd components at three times (with  $t_{ZK} = 3.6t_B$ ). The additional line at  $t = 3.1t_B$  is for showing the signature of the ninth weakest soliton (rather than the radiating signal [10])

Fig. 4 presents the velocity profiles, precisely those of ZK65, and their even/odd components defined before, with the wavenumbers normalized accordingly to be integers. Some observations follow. Consistent with the initial condition, the corresponding even-velocities are actually of unit period, i.e.,  ${}^e u(x, t) = {}^e u(x + 1, t)$ , and odd-velocities of “unit anti-period”, in the sense that within the period  $L_p = 2$ ,  ${}^o u(x, t) = -{}^o u(x + 1, t)$ .  ${}^e u$  tends to form shocks at both  $x_B = 1$  and  $x'_B = 3/2$  at the inviscid-Burgers blow-up time  $t_B (= 1/\pi$  now), before evolving into soliton-like structures, and  ${}^o u$  to shock and anti-shock (or steep “kink”, as used to describe the topological soliton of the sine-Gordon equation [33]), respectively at  $x = 1$  and  $x = 3/2$ . Once they evolve into solitary pulses,  ${}^e u$  and  ${}^o u$  present similar features in their patterns, which however is not the case for the alternating-dispersion models to be presented below. They are not as solitary as real solitons, as indicated by the comparisons of their space-time contour plots (with still somewhat trackable space-time characteristics though) to that of the undecomposed  $u$ . Such characteristics are of course case specific, but still helpful. What appears remarkable is that  ${}^{e/o}(u \partial_x u)$  tend to produce (anti)shocks at both  $x_B = 1$  and  $x'_B = 3/2$ , even starting from the null field for  ${}^e u$ . The oscillations all emerge and develop, as already indicated by the nascent ones at  $t_B$  and other later ones (not shown) following them, behind the (anti)shocks, with the linear waves of both branches supposed to propagate backward with phase velocities  $-k^2$ . Though not accomplished here, one of our motivations of inspecting such decomposed fields is to offer a comparison with those of aKdV below.

### 3.2. Even-odd alternating dispersion: shock, soliton and shocliton

Fig. 5 presents the velocity profiles of the even-odd-alternating-dispersion KdV equation with decreasing  $\mu = \pm {}^e \mu = \mp {}^o \mu$  from left to right, showing, just as the classical KdV, increasing oscillations on both sides of the (anti)shocks. So, we have seen not only the objective of mimicking the two-sided oscillations observed in some plasma and quantum shocks but also the singular behavior as an indication of nonconvergence to the classical shock described by an entropy solution. We reiterate that such two-sided oscillations for given  $\mu$  are not the Gibbs phenomena but “physical”.

Fig. 6 presents  ${}^{e/o}u$  of the case with  ${}^e \mu = -{}^o \mu = \delta^2$ . [The other cases are accordingly similar and not shown.] As expected, the profiles are close to the corresponding ones in Fig. 4 for KdV at  $t \leq t_B$ , but  ${}^{e/o}u$  are quite different at  $t = 3.6t_B$  after the differences in the dispersions take more and more effect: for instance, the plateau-basin structure of  ${}^o u$  of the aKdV is even strengthened (and persistent — see below), instead of broken into “simple” solitary pulses in the fashion of the KdV case.

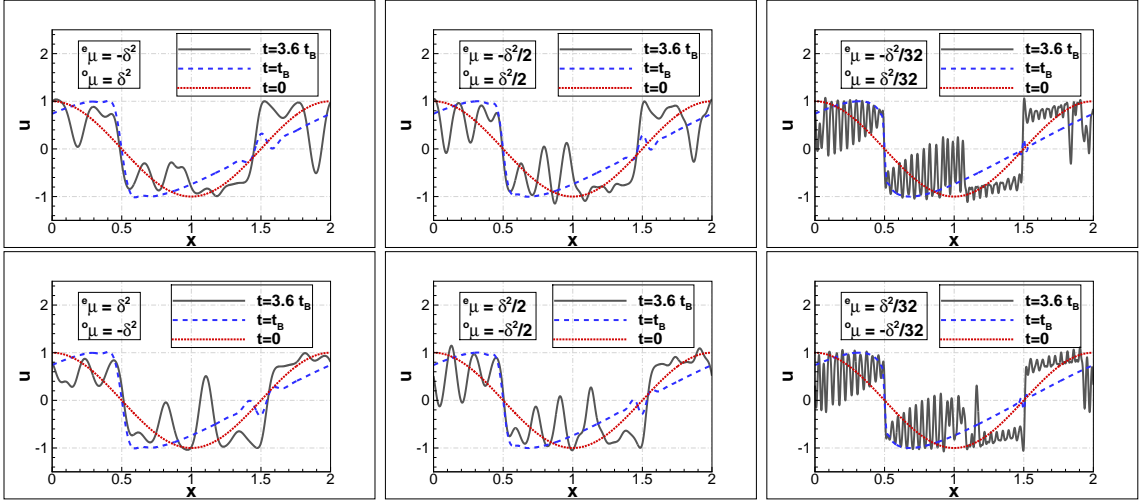


Figure 5: Velocity profiles of aKdV with different parameters.

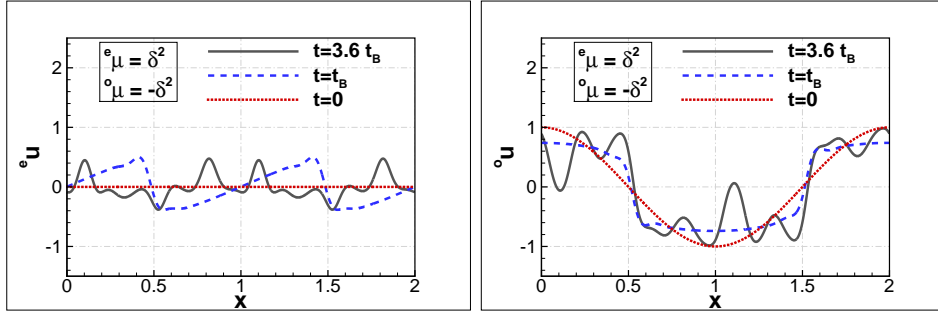


Figure 6:  $e/o_u$  of aKdV.

Note that besides the shock at  $x = 1/2$  as in KdV, the other anti-shock emerges at  $x = 3/2$ , and on both sides of the respective shock live the oscillations of close features (Fig. 5). Drastically different amplitudes of the oscillations around the respective shock can present (Fig. 5), but not always (Fig. 7 for  $\mu = \delta^2/8$ ). The overall scenario is that the oscillations are “solitary”, which will become more obvious in the observation of Fig. 8 below. And, we also see slight leftward shift or slowly travelling of the (anti)shocks, due to the small difference between  ${}^o\tilde{D}$  and  ${}^e\tilde{D}$  coming from that of the alternating even and odd wavenumbers: as already can be seen from the comparison between the upper and lower rows of Fig. 5 and checked by the long-time contour patterns, when the signs of the even and odd dispersion coefficients are reflected to opposite signs, the (anti)shocks of the two cases travel with opposite but same-amplitude speeds. Actually, as particularly clear at  $t = 6t_B$ ,  $9.6t_B$ ,  $12t_B$ ,  $18t_B$  and  $19.2t_B$  for instance, the (anti)shocks seem to be “unifiable” into the oscillations: A rigorous and formal mathematical description is lacking, and the issue will become clearer with more insights motivated by the properties of the transported particles to be studied in a different communication. It appears then reasonable to raise the notion of “(anti)shock-soliton” or, probably even more precisely, “(anti)shocliton” as a mixture of (anti-)shock and soliton to indicate the continuous transition between an (anti-)shock<sup>2</sup> and a (normal) soliton.

The obvious feature of the persistent but slowly drifting plateau-basin structure carrying the smaller oscillations on both sides of the (anti)shocks is maintained by  ${}^o u$  (c.f. Fig. 6) in this case, while  ${}^e u$  presents

<sup>2</sup>The “shock” in this note however should be distinguished from the shock “soliton” [34, 10] of viscous Burgers equation, so the notion of duality or “shocliton” is not trivial. The other oscillations not of shock feature will be called “normal” solitons.

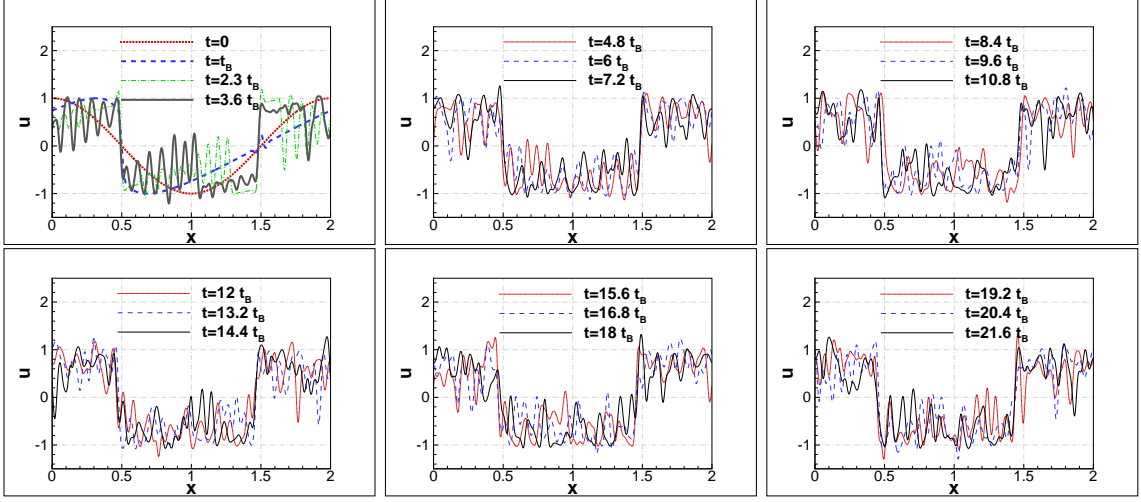


Figure 7: Velocity profiles of aKdV at various times with  $\mu = \varrho\mu = -\epsilon\mu = \delta^2/8$  and  $\delta = 0.022$ .

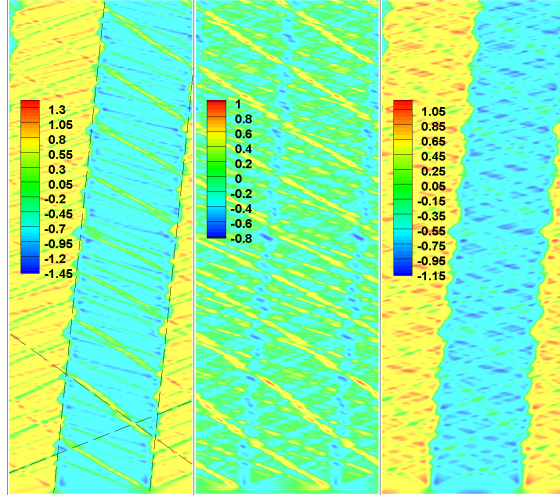


Figure 8: Contours of  $u$  (left frame),  $\epsilon u$  (middle) and  $\varrho u$  (right) for aKdV with  $\epsilon\mu = \mu = -\varrho\mu$ , respectively for  $t \leq 20t_{ZK}$  (with four black dashed lines added to highlight the corresponding characteristics, two longest ones of them respectively for the shoeliton and antishocliton).

more of soliton feature, which is similarly followed by the other cases to be presented below. The conjecture, that the oscillations of such aKdV equation are solitons, appears to be supported by the contours presented in Fig. 8 where the (straight) “bars” coded by the same-level colors indicate the characteristics along which the solitary waves are travelling with collisions (interactions) resulting in some phase shifts: we indeed see there are “bars” of different slopes, indicating different velocities of the solitons, and their collisions seem to be weaker than those of the KdV equation in Fig. 4; careful inspection shows that the bars/characteristics (for solitons as conjectured by us) pass through the (anti)shoclitons which also travel at nearly (but probably not precisely) constant speeds as clearly shown by their characteristics over the time up to  $80t_{ZK}$ ,<sup>3</sup> supporting again the “soliton-shock duality”. The pattern appears to contain some disorder, which may be described as

<sup>3</sup>The penetration and continuation of the characteristics of the conjectured solitons across the (anti)shoclitons become much less trackable in the uniform color coding, due to the obvious jumps of the  $u$ -levels from the shock-property of the (anti)shoclitons.

“pseudo-periodic”, with the structures at most quasi- or almost-periodic. This is similar to the “longlunt states” of the Galerkin regularized/truncated systems [31, 32], with clear indication of the whiskered tori, and accordingly the notion of pseudo-integrability in terms of carrying a proper set of on-torus invariants [ $\mathcal{H}$  and  $\mathcal{I}_\tau$  in Eq. (2.25)] which precisely specify the state.

From the soliton point of view, such “shoclitons” present at the top and bottom anti-directional overshoots (compared to the respective average plateau/basin profiles further away from the jumps), thus characterized to be “big but weak” (“weak” for the strength averaged over the two sides). The anti-directional overshoots on the two sides of such a shock sum up to constitute the amplitude of the (weak) soliton identity, consistent also with the specification of the classical limiting shock velocity  $u_s = (u^+ - u^-)/2$  (for quadratic nonlinearity here [35]) where  $u^+$  and  $u^-$  are the left- and right-limit velocities of the ideal (entropy) shock. Being “weak”, the velocities of such solitons are then presumably very small, as shown by the slopes of their characteristics. Note that the (anti)shocliton phase shifts due to the collisions with solitons from both sides can not cancel overall, due to the differences of the other counter propagating solitons (from the even-odd asymmetry in the nonlinear and linear terms).

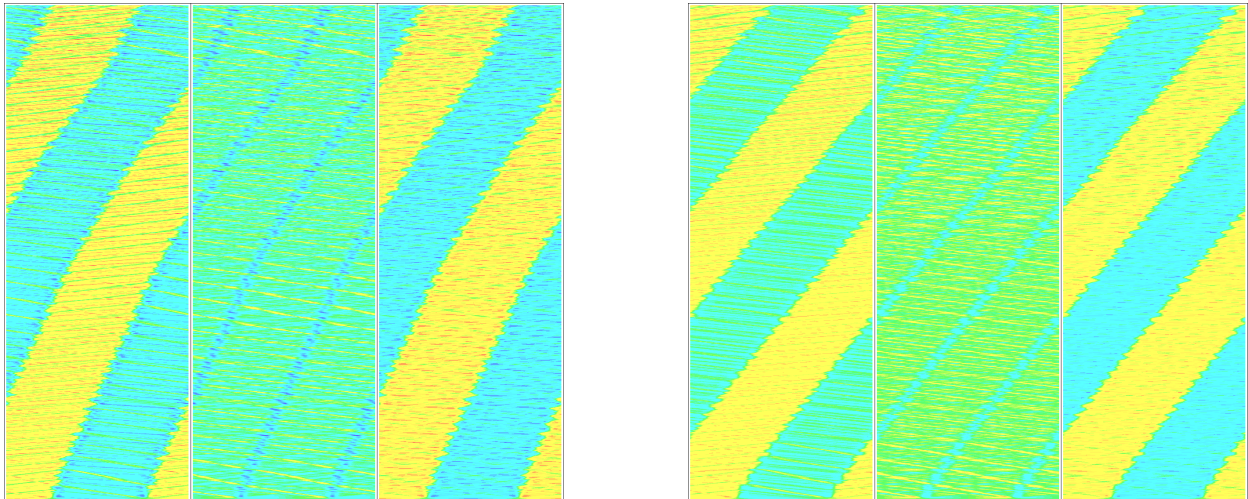


Figure 9: Contours of  $u$  (left frame),  ${}^e u$  (middle) and  ${}^o u$  (right) for the aKdV (left panel) and accordingly those from the “corrected” aKdV (right panel), with  ${}^e \mu = \mu = -{}^o \mu$ ; both for  $t \leq 80t_{ZK}$ .

There is slight deviation from constancy of the velocity of the “(anti)shoclitons” (not clear to our bare eyes for  $t \leq 20t_{ZK}$  in Fig. 8, but marked in the left panel of Fig. 8 for  $t \leq 80t_{ZK}$ ). We have noticed the even-odd asymmetry in the wave dispersion and proposed the correction recipe with Eq. (2.29) for the alternating dispersion function which, as shown in Fig. 9 (right panel) by the computation with everything else the same, works perfectly to have a corrected constant drifting velocity: this in turn indicates that the deviation from the constant drifting speed of the numerical result for the uncorrected model be genuine, not due to numerical errors.

### 3.3. Driven-damped case

Like tuning the spin-orbit coupling of BECs [3, 4, 5] to engineer the dispersions, we can also accordingly design the latter in our aKdV models. Note that it is trivial to include the diffusive term to have our alternative-dispersion KdVB (aKdVB), and, according to the connection with quantum shocks [36], the corresponding two-sided oscillations may be associated to those found in BEC [5]. Our alternating-dispersion idea for the two-sided oscillations of the shock of course belongs to the nonconvex dispersion like the Kawahara model [6, 7], but is different to the latter, most obviously in their orders. Additional specific studies are needed to see which dispersion model is more appropriate for a particular physical system.

The aKdVB with appropriate diffusion (and forcing, if needed, say, for stationarity) can still produce the (anti)shocliton, and we should note particularly that, concerning the oscillations on both sides of the

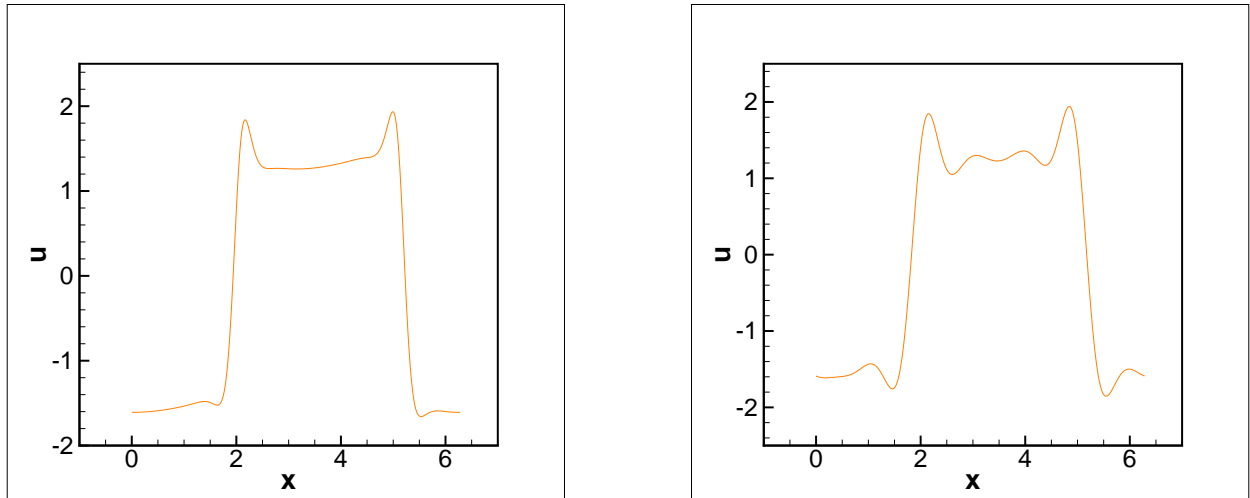


Figure 10: The aKdVB results with  $m = 1$  (left:  $\nu = 0.018/2$  and  $\mu = 0.024/2$ ) and  $m = 2$  (right:  $\nu = 0.018/2$  and  $\mu = 0.001/2$ ).

(anti-)shock, the numerical KdVB shocks with only one-sided oscillations in Ref. [1] actually could not qualitatively explain the experimental results therein, and further efforts of modelling are necessary. Now, we consider the aKdVB model

$$\{\partial_t + \nu k^2 - \hat{\mu} i k^{2m+1} [\text{mod}(k, 2) - \text{mod}(k+1, 2)]\} \hat{u}_k = \hat{f}_k - \hat{i} \sum_{p+q=k} \hat{q} \hat{u}_p \hat{u}_q. \quad (3.2)$$

Using the forcing  $f(x) = (\sin x)/4$ , two snapshots in the (quasi-)stationary stage from simulations over a  $2\pi$  period, respectively with  $m = 1$  and  $m = 2$  (“hyperdispersion” mentioned earlier), as presented in Fig. 10, indeed have (anti)shockltons with two-sided oscillations, but, unlike the aKdV ones in Figs. 5 and 7, with the oscillations far away from the shock being reasonably smoothed out by the diffusion term, thus closer to the ion-acoustic shocks measured in laboratory experiment of Ref. [1]. Instead of fixing  $m = 1$  and tuning  $\mu$  and  $\nu$ , we have used  $m = 2$  to obtain different oscillation features. Note that, like the aKdV case, the aKdVB shocklton and antishocklton in Fig. 10 do not collide but be constantly separated.

The shocklton-antishocklton dyad presents also in other models other than aKdV, including acutally those who even do not have explicitly apparent linear dispersive terms such as GrBH [31]. The sine-Gordon equation without or with appropriate perturbations admits the “kink-antikink” pair (e.g., Refs. [37, 38]), and similarly the “kovaton” [39], which morphologically resembles our case except that, to the best of our knowledge, no oacillations around them have been studied.

### 3.4. Nonlinear quantum revival and fractalization

We now test the aKdV FaQR, for good comparisons to the LaKdV FaQR in Sec. 2.3.1 (with the same setup except for the nonlinear term), to the shockltons from the sinusoidal data in Sec. 3.2, and to the KdV results of Chen and Oliver [21] (with the same setup except for the signs of the nonlinear and dispersion terms).

Fig. 11 shows the aKdV FaQR. The fractalization feature is similar to that of LaKdV (with no visible essential differences to our bare eyes) in Sec. 2.3.1, thus not shown and left for future studies on particle transports sensitive to the very fine details. The FaQR profiles seemingly look quite different, as in the linearized case, but overall they actually preserve the shock-antishock structure quite well, as shown by the carpet in Fig. 12. Interestingly, we have checked that such a scenario is present in the corresponding KdV results as well, with only minor differences in the details. [In other words, Chen and Olver should have also observed it.] The reason is that the shock-antishock structure, preserved also by the KdV dispersion,

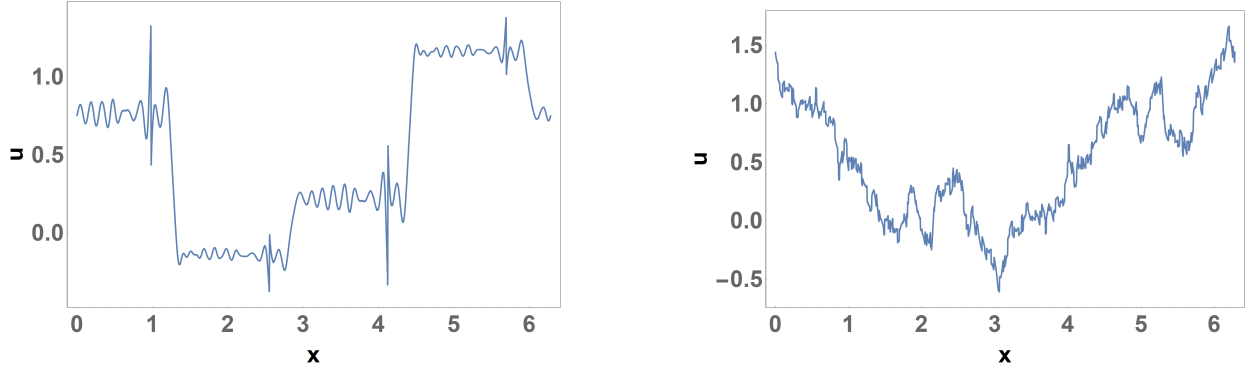


Figure 11: The aKdV quantum revival at a rational time (left) and fractalization at an irrational time (right).

is mainly composed of odd- $k$  modes, with the minor oscillations about the plateau and valley containing even- $k$  modes (excited by nonlinear interactions). This is different to the linear case in Sec. 2.3.1 with no nonlinear interactions to excite the even- $k$  modes, thus no difference between aKdV and KdV. [As remarked in the introductory discussions, the quantum revival panel in Fig. 11 also presents spikes, like those in Farmakis et al. [24] whose used the cubic nonlinearity to replace the quadratic one in Eq. (1.1).]

The carpet contains fine bands indicating very fast waves/solitons, i.e., the minor oscillations, going across plateau and valley separated by the constantly drifting shock and antishock. The shock travelling velocity is not the standard shock velocity  $1/2$  as the mean of the original step function, so the (anti)shock indeed drifts additionally, actually at a speed of around  $1.5$ , the value as the sum of the standard shock velocity ( $1/2$ ) and the linear wave velocity of  $|k| = 1$ . The initial step data with zero mean velocity also result in additional shock drifting (not shown), similar to those starting with cosine data presented earlier. With the dispersion coefficient  $1 \gg \delta^2$ , the drifting here is marked compared to that in Sec. 3.2. So, aside from the fractalization and quantum revival, the scenario is similar to what we have observed in the previous case starting from sinusoidal initial data. With FaQR, the remarkable footprints of linear waves should not be surprising.

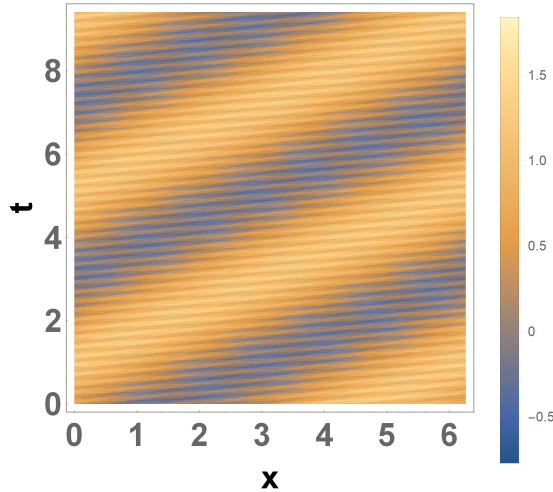


Figure 12: FaQR carpet: besides the major structures carried by (anti)shocks, fine bands of fractalization and quantization waves are clear.

So, we have found a kind of unification/consistency between aKdV soliton(-like) behavior and FaQR. Actually, the shock-antishock structure is also preserved in GrBH [31], with neither the additional drifting

nor the fractalization-quantum revival phenomena though, indicating some connections and even wider unification/consistency, as already remarked in Sec. 2.3.1.

#### 4. Concluding discussions

This research project started from the simple observations, on the one hand, that Gardner’s variational formulation and Hamiltonian structure for KdV may be equally powerful for different pseudo-differential (Fourier mode dependent) variations, such as the reassignment of linear frequencies or even the truncation of nonlinear-advection dispersion, and, on the other hand, that new dispersion by alternating the signs of the linear frequencies of the neighboring wavenumbers could well be able to simulate the wave-like pulses oscillating on both sides of the shocks, observed in some plasma and quantum mediums but not in KdV results.

Systematically carrying out the program with the aKdV model, we have not only established the above two points, with extended results such as the driven aKdVB shocks to have a broader and more concrete ground, but also discovered solitonic structures with pseudo-periodic patterns. Bearing some genericity for nonintegrable conservative systems (simultaneously supported by the discoveries of Gr-systems with the truncation resulting in nonlinear dispersion [31] — see below), the latter probably is fundamentally more important and motivating.

We have also checked the applicability of the idea in modified KdV model with cubic nonlinearity, and also other models and its extensions, all (not shown) with similar scenarios concerning the shock-antishock and close oscillations on both sides.

The above aKdV model can be viewed as adding a modification dispersion (twice the opposite of the original dispersion which is modified, otherwise zero) to the original KdV dispersion. The nonlinear advection term in the KdV equation can also be viewed as a nonlinear dispersion, and similar reassignment of the nonlinear dispersion or addition of a correction dispersion is actually realized by the familiar Galerkin truncation/regularization: consider for simplicity the dispersionless KdV, i.e., the Burgers-Hopf equation  $\partial_t v + \partial_x v^2/2 = 0$  and the regularized (GrBH) dynamics [40, 31]

$$\partial_t u + u \partial_x u = {}^K g; \quad u_0 = P_K \{v_0\}; \quad (4.1)$$

$${}^K g = (I - P_K) \{u \partial_x u\} = \sum_{\substack{p+q=m \\ |p|, |q| \leq K < |m|}} \hat{u}_p \hat{u}_q e^{imx}, \quad (4.2)$$

where  $P_K \{v(x)\} = \sum_{|k| \leq K} \hat{v}_k \exp\{ikx\}$  with  $\hat{v}_n$  being the conventional Fourier coefficient of variable  $v$  at wavenumber  $n$  ( $\hat{v}_n^* = \hat{v}_{-n}$  for reality) and where  $v_0$  is the initial data. That is, use is made of the projection onto the Fourier space with  $-K \leq |k| \leq K$  (“Galerkin space” hereafter) for some integer  $K$ . Such  $u$  stays initially, and forever, in the Galerkin space which is thus dynamically “complete”. So, we see that the reassignment of the nonlinear dispersion is realized by the Galerkin dispersion  ${}^K g_m$  which is opposite to the original nonlinear dispersion for  $|m| > K$ . [We have used different notations, such as  $k$  and  $m$  for distinguishing different wavenumber regimes.] Like aKdV, such a system preserves the invariance of energy and Hamiltonian inherited from the classical KdV system [28, 41].

The addition of opposite dispersion appears to be the common mechanism of maintaining the (dispersive) shocks from sinusoidal initial data in both aKdV (see below) and GrBH [31]. In the aKdV case, the physics is that the unidirectional dispersion is counterbalanced by the opposite directional dispersion of waves, while in the GrBH case, the nonlinear dispersion, leading otherwise to singularity, is counterbalanced by opposite small-scale self-advection, which can be consistently approximated by a unidirectional small-scale linear wave dispersion [31]. Such a comparison can be mutually illuminating: indeed we were partly led by current work to revisit Gr-systems with new discoveries which then in turn motivate further aKdV progresses here, including to similarly propose the on-torus aKdV invariants which may lead to relevant quasi- or even almost-periodic orbits, in a way similar to the integrable KdV case. Such problems of nonintegrable systems, with the systematic solutions sounding far beyond the state-of-the-art of nonlinear science though,

is fundamentally interesting and practically useful (reality are usually not integrable with still with solitonic structural dynamics).

The robustness of the FaQR in such manipulated aKdV model is intriguing, and, together with the unified/consistent ubiquitous features of oscillations caused around a shock, motivating thoughts about the fundamental mechanism and applications. For example, as also hoped in Ref. [20], understanding the fractalization is an attractive project in the field and may benefit from the quantitative differences of KdV and aKdV; and, the particle transport, especially the aggregation/condensation, is sensitive to fractalization and shocks/quantization, which is a subject of on-going further studies.

## References

- [1] Y. Nakamura, H. Bailung and P. Shukla, Observation of Ion-Acoustic Shocks in a Dusty Plasma. *Phys. Rev. Lett.* **83**, 1602–1605 (1999).
- [2] J. Huang et al., Ion Acoustic Shock Wave Formation and Ion Acceleration in the Interactions of Pair Jets with Electron–ion Plasmas. *The Astrophysical Journal* **931**, 1 (2022).
- [3] Y.-J. Lin, R. L. Compton, K. Jimenez-Garcia, J. V. Porto, and I. B. Spielman, Synthetic magnetic fields for ultracold neutral atoms, *Nature* **462** 628–632 (2009).
- [4] Y.-J. Lin, K. Jimenez-Garcia, and I. B. Spielman, Spin-orbit-coupled Bose-Einstein condensates, *Nature* **471**, 83–86 (2011).
- [5] M. E. Mossman, E. S. Delikatny, Michael McNeil Forbes, and P. Engels, Stability in turbulence: The interplay between shocks and vorticity in a superfluid with higher-order dispersion. *Phys. Rev. A* **102**, 053310 (2020).
- [6] P. Sprenger, M. A. Hoefer, Shock waves in dispersive hydrodynamics with nonconvex dispersion. *SIAM J Appl Math.* **77**, 26–50 (2017).
- [7] M. A. Hoefer, N. F. Smyth, P. Sprenger, Modulation theory solution for nonlinearly resonant, fifth-order Korteweg-de Vries, nonclassical, traveling dispersive shock waves. *Studies in Applied Mathematics* **142**, 1 (2018).
- [8] N. J. Zabusky and M. D. Kruskal, Interaction of “Soliton” in a Collisionless Plasma and the Recurrence of Initial States, *Phys. Rev. Lett.* **15**, 240 (1965).
- [9] C. S. Gardner, J. M. Greene, M. D. Kruskal, and R. M. Miura, Method for solving the Korteweg-de Vries equation, *Phys. Rev. Letters* **19**, 1095–1097 (1967).
- [10] A. R. Osborne, *Nonlinear Ocean Waves and the Inverse Scattering Transform*, International Geophysics Series, Vol 97, Elsevier/Academic Press (2010).
- [11] K. T-R McLaughlin and P. V. Nabelek, A Riemann–Hilbert Problem Approach to Infinite Gap Hill’ s Operators and the Korteweg–de Vries Equation, *International Mathematics Research Notices*, **00**, 1 – 65 (2019).
- [12] P. Suret, S. Randoux, A. Gelash, D. Agafontsev, B. Doyon, and G. El, Soliton Gas: Theory, Numerics and Experiments. *Phys. Rev. E* **109**, 061001 (2024).
- [13] H. F. Talbot, Facts related to optical science. **IV**, *Philos. Mag.*, 401 – 407 (1836).
- [14] M.V. Berry, and S. Klein, Integer, fractional and fractal Talbot effects, *J. Mod. Optics* **43**, 2139 – 2164 (1996).
- [15] I. Rodnianski, Fractal solutions of the Schrödinger equation, *Contemp. Math.* **255**, 181 – 187 (2000).
- [16] M. V., Berry, I. Marzoli, and W. Schleich, Quantum carpets, carpets of light, *Physics World* **14**, 39 – 44 (2001).
- [17] Y. Zhang, J. Wen, S. N. Zhu, and M. Xiao, Nonlinear Talbot effect. *Phys. Rev. Lett.* **104**, 183901 (2010).
- [18] P. J. Olver, Dispersive quantization, *Amer. Math. Monthly* **117** 599 – 610 (2010).
- [19] M. B. Erdogan and G. Shakan, Fractal solutions of dispersive partial differential equations on the torus, *Selecta Math.* **25** 11 (2019).
- [20] P. J. Olver, E. Tsatis, Points of constancy of the periodic linearized Korteweg–deVries equation. *Proc. R. Soc. A* **474**, 20180160 (2018).
- [21] G. Chen and P. J. Olver, Numerical simulation of nonlinear dispersive quantization, *Discrete Contin. Dyn. Syst.* **34**, 991 – 1008 (2014).
- [22] V. Chousionis, M. B. Erdogan, N. Tzirakis, Fractal solutions of linear and nonlinear dispersive partial differential equations. *Proc. Lond. Math. Soc.* **110**, 543 – 564 (2015).
- [23] D. A. Smith, Revivals and Fractalization, *Dyn. Sys. Web* **2020**, 1 – 8 (2020).
- [24] G. Farmakis, J. Kang, P. J. Olver, C. Qu, and Z. Yin, New revival phenomena for bidirectional dispersive hyperbolic equations. [arXiv:2309.14890 \[math.AP\]](https://arxiv.org/abs/2309.14890).
- [25] V. E. Zakharov, On the stochastization of one-dimensional chains of nonlinear oscillators. *Sov. Phys. JETP* **38**, 108 – 110 (1974).
- [26] S. K. Turitsyn, Blow-up in the Boussinesq equation. *Phys. Rev. E* **47**, R796 (1993).
- [27] R. L. Sachs, On the Blow-up of Certain Solutions of the “Good” Boussinesq Equation, *Applicable Analysis: An International Journal* **36**, 145 – 152 (1990).
- [28] C. S. Gardner, Korteweg-de Vries Equation and Generalizations. IV. The Korteweg-de Vries Equation as a Hamiltonian System, *J. Math. Phys.* **12**, 1548 (1971).
- [29] S.P. Novikov, The periodic problem for the Korteweg-de Vries equation, *Funct. Anal. Appl.* **8**, 236–246 (1974).
- [30] P. Lax and J. M. Hyman, Periodic Solutions of the KdV Equation. *COMMUNICATIONS ON PURE AND APPLIED MATHEMATICS, VOL. XXVIII*, 141-188 (1975).
- [31] J.-Z. Zhu, Travelling-wave, Quasi-periodic, Longlent States and Persistent Whiskered Tori of the Galerkin-regularized Systems, preprint (2024); J.-Z. Zhu, Longons from the nonlinear dispersion of Galerkin regularization, preprint (2024).



- [32] J.-Z. Zhu, “Constructing longlulent states of the Galerkin-regularized nonlinear Schrödinger and complex Ginzburg-Landau systems”, preprint (2024).
- [33] M.J. Ablowitz, H. Segur, *Solitons and the Inverse Scattering Transform*, SIAM, Philadelphia, 1981.
- [34] S. Wang, X. Y. Tang, S. Y. Lou, Soliton fission and fusion: Burgers equation and Sharma-Tasso-Olber equation, *Chaos Solitons Fractals* 21, 231–239 (2004).
- [35] G. B. Whitham, *Linear and Nonlinear Waves*. Wiley, New York (1974)
- [36] M. Kulkarni and A. G. Abanov, *Phys. Rev. A* 86, 033614 (2012).
- [37] A. Sanchez, R. Scharf, A. R. Bishop, and L. Vazquez, Sine-Gordon breathers on spatially periodic potentials, **45**, 6031 (1992).
- [38] H. Zhang and Y. Xia, Persistence of the kink and anti-kink wave solutions for the perturbed double sine-Gordon equation, *Applied Mathematics Letters* **141**, 108616 (2023).
- [39] P. Rosenau and A. Pikovsky, Phase Compactons in Chains of Dispersively Coupled Oscillators, **94**, 174120 (2005).
- [40] E. Tadmor, Convergence of spectral methods for nonlinear conservation laws. *SIAM J. Numer. Anal.* **26**, 30 (1989).
- [41] R. Abramov, G. Kovačič, and A. J. Majda, Hamiltonian Structure and Statistically Relevant Conserved Quantities for the Truncated Burgers-Hopf Equation. *Comm. Pure Appl. Math.* **LVI**, 0001 (2003).